Capillary Condensation in a Fractal Porous Medium

Daniel Broseta,* Loïc Barré, and Olga Vizika
Institut Français du Pétrole, 92842 Rueil-Malmaison Cedex, France

Noushine Shahidzadeh and Jean-Pierre Guilbaud
Laboratoire des Matériaux et Structures du Génie Civil, 2 allée Kepler, 77420 Champs/Marne, France

Sandrine Lyonnard
Service de Chimie Moléculaire, CEA/Saclay, 91191 Gif sur Yvette Cedex, France
(Received 17 August 2000; revised manuscript received 10 January 2001)

Small-angle x-ray and neutron scattering are used to characterize the surface roughness and porosity of a natural rock which are described over three decades in length scales and over nine decades in scattered intensities by a surface fractal dimension $D = 2.68 \pm 0.03$. When this porous medium is exposed to a vapor of a contrast-matched water, neutron scattering reveals that surface roughness disappears at small scales, where a Porod behavior typical of smooth interfaces is observed instead. Water-sorption measurements confirm that such interface smoothing is due predominantly to the water condensing in the most strongly curved asperities rather than covering the surface with a wetting film of uniform thickness.

DOI: 10.1103/PhysRevLett.86.5313 PACS numbers: 68.08.–p, 61.10.Eq, 61.12.Ex, 68.35.–p

Sedimentary rocks are one of the most extensive fractal systems found in nature [1]. The surface roughness and porosity of these natural porous media are in many instances adequately described, over length scales that may range from the nanometer to a few microns, by a single, nonuniversal fractal dimension D ($2 < D < 3$), where D approaches 2 for smooth, clay-free rocks, while values close to 3 are typical of strongly argillaceous sandstones [1–3]. Organic porous media such as coals also exhibit surface fractality [4]. The complex geochemical processes that lead to such remarkable self-similar properties are not yet understood [3].

These observations hold for *dry* porous media. The present Letter addresses the situation, relevant to hydrology and petroleum reservoir engineering applications, where the fractal porous rock is partially invaded by a wetting fluid (e.g., water), the third, nonwetting phase being the vapor. This Letter presents a series of small-angle scattering experiments on *wet* fractal rocks that provide, for the first time, a direct visualization (in the Fourier reciprocal space) of fluid distribution within the fractal rock substrate. These experiments unambiguously show that the presence of the wetting fluid has for effect to smooth the substrate on the smaller length scales. The new lower limit of fractality is identified as the maximum radius of filled surface concavities.

There are basically two limiting regimes for wetting fluid distribution within the pore space (for a review, see Ref. [5]). When capillary forces are important, as it turns out to be the case for the experimental system of this study, the wetting fluid is primarily located in the most strongly curved surface concavities. Such a *capillary wetting* regime is encountered for significant substrate irregularity (as quantified, for fractals, by D), high enough wetting fluid content, and large enough surface tension. In this regime, the relevant length scale is the maximum radius of curvature of filled concavities (denoted R below). In the other limiting regime, corresponding to strong fluid/substrate interactions, the wetting fluid is primarily located in wetting films covering the whole substrate and having homogeneous thickness. This *substrate-controlled* wetting regime is encountered for smooth substrates (small D), low wetting fluid content in the porous medium, and strong substrate/adsorbate interactions. The characteristic length in this case is the film thickness (denoted d below).

Small-angle scattering experiments with a wetting fluid contrast matched with the porous substrate have been proposed and discussed in the 1980s by de Gennes [6] for systems in the capillary wetting regime and by Cheng, Cole, and Pfeifer [7] for systems in the substrate-controlled wetting regime. These authors anticipated a crossover for the scattered intensity from a fractal behavior at large length scales (small scattering vectors q) identical to that of the dry material, to a Porod-like behavior typical of smooth surfaces at small length scales (large q), with the crossover scattering vector corresponding to the inverse characteristic length $q^* \approx 1/R$ or $1/d$, depending on the fluid distribution regime.

The experiments consisted in first characterizing the fractal nature of the dry porous medium by means of both small-angle x-ray and neutron scattering. The wetting fluid (a H_2O/D_2O mixture with a minimum neutron contrast with the rock) was then introduced into the porous medium to various controlled degrees by exposure to undersaturated vapors. These wet samples have been analyzed by small-angle neutron scattering (SANS), thus characterizing the wetting fluid distribution in the porous structure. In order to assess the fluid distribution regime, conventional water-sorption measurements have also been performed.

 © 2001 The American Physical Society

The porous rock is a Vosges sandstone of porosity $\phi = 0.17$ and permeability $k \approx 5 \times 10^{-14}$ m^2. All its constituents (with the exception of 1% hematite) [8] have nearly identical scattering length densities for both x rays ($\approx 0.8\ e^-/\text{Å}^3$) and neutrons ($\approx 4 \times 10^{-6}$ Å^{-2}), which ensures the validity of the two-component (i.e., rock and air) approximation for interpreting the data. The SANS instrument used (from Laboratoire Léon Brillouin, CEA/Saclay) covers a range of scattering vectors, $3 \times 10^{-3} < q < 0.2$ Å^{-1}. The x-ray instrument used is a double crystal Bonse-Hart camera designed for measurements at ultrasmall angles ($3 \times 10^{-4} < q < 0.2$ Å^{-1}). The range of sizes $1/q$ probed by these instruments thus extends from ≈ 5 Å to around 0.03 μm with SANS and 0.3 μm with small-angle x-ray scattering (SAXS). Rocks being much more adsorbent to x rays than to neutrons, slices with thicknesses much larger for SANS (1.6 mm) than for SAXS (0.23 mm) were used.

Figure 1 shows the measured SAXS and SANS absolute intensities, normalized by the respective contrast terms (i.e., by the squared scattering length densities of the rock). These intensities display over the whole range of q a power-law behavior typical of surface fractals [9]:

$$I(q) = Aq^{-\alpha} + B, \quad (1)$$

where the exponent α is related to the surface fractal dimension D: $\alpha = 6 - D$; A is related to the quantity of interfaces present in the rock material [see below Eq. (2)]; and B represents the incoherent background (for neutrons only).

Excellent agreement between the SAXS and SANS data is found in the overlap region ($q > 3 \times 10^{-3}$ Å^{-1}). The exponent $\alpha = 3.32$ and therefore $D = 2.68$. The SAXS data cover nearly three decades in length scales and over nine decades in intensities. SANS spectra were obtained for five different rock slices. A nonlinear least-squares analysis of these spectra using Eq. (1) yields values for α ranging from 3.31 to 3.35, from which we estimate that $\alpha = 3.32 \pm 0.03$ and $D \approx 2.68 \pm 0.03$.

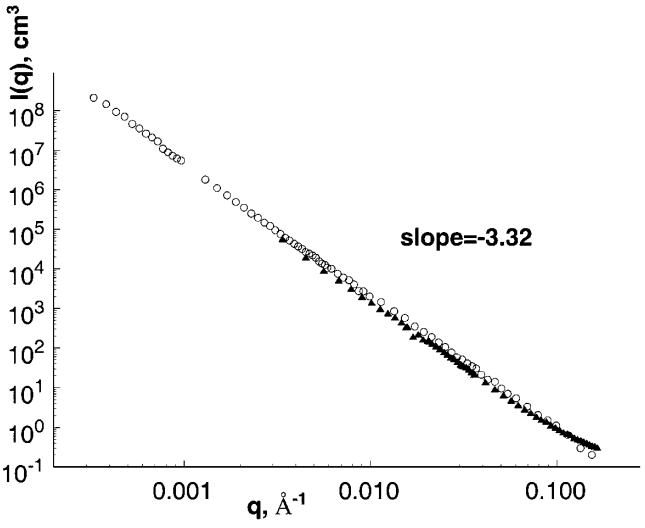

FIG. 1. SAXS (circles) and SANS (triangles) intensities of a Vosges sandstone, normalized by the relevant contrast term.

The coefficient A in Eq. (1) can be related directly to the quantity of interfaces present in the porous material, by [10]:

$$A = \pi \sigma_x \rho \Gamma(5 - D) \sin[(3 - D)\pi/2]/(3 - D), \quad (2)$$

where ρ is the mass density (=2.3 g/cm^3), Γ the gamma function, and σ_x the prefactor relating the specific surface area of the surface fractal, σ, to the length scale R of the measurement, i.e., $\sigma = \sigma_x R^{2-D}$. From the small-angle scattering data, we find $\sigma_x \approx 0.8$ cm^D/g, which would correspond to a specific surface area for coverage with krypton gas (molecular cross-sectional area $R^2 \approx 20.2$ Å^2) of $\sigma \approx 7$ m^2/g. We have carried out a Brunauer-Emmett-Teller (BET) adsorption measurement with krypton gas and obtained a specific area of ≈ 3.5 m^2/g. Small-angle scattering thus provides the correct order of magnitude for σ. The difference between the two values might be due to multiple scattering effects: Radlinski *et al.* [1] have shown that for similar sedimentary rocks it is necessary to reduce the thickness of samples to below 1 mm in order to have negligible multiple neutron scattering. On the other hand, some of the pores might be inaccessible to the gas molecules, leading to a lower area in the BET adsorption measurements.

Subsequently, the SANS experiments on wetted porous media were carried out by using a wetting H_2O/D_2O mixture, the composition of which (68.6 wt.% D_2O) minimizes the scattering contrast with the rock. Therefore, the rock-water interfaces are invisible to the scattering process. The water was introduced in the porous medium as follows. The rock slices, initially imbibed with the wetting fluid, were left in contact (in a dessicator) for a few days with the vapor of a water liquid phase saturated with a given salt. In this process, some of the liquid water in the porous medium evaporated, down to an equilibrium value S_w (S_w is the proportion of the porous space occupied by the wetting fluid). The salts used, NaCl, KNO_3, or K_2SO_4, allowed us to lower the vapor pressure P below that of pure water P_{sat} in a controlled fashion and thus to impose within the rock slices the Kelvin capillary pressure,

$$P_c(S_w) = -\frac{RT}{v} \log(P/P_{\text{sat}}), \quad (3)$$

with T the temperature, $R = 8.314$ J/K, and v the liquid water molar volume. Then, using literature values for relative humidities P/P_{sat}, capillary pressures at the temperature of the experiment ($T = 21 \pm 1$ °C) are calculated to be $P_c \approx 383$ bars (NaCl), 100 bars (KNO_3), and 35.9 bars (K_2SO_4). The corresponding final fillings S_w, measured by weighing, were, respectively, $S_w = 5.0\% \pm 0.6\%$, $12.0\% \pm 1.2\%$, $14.2\% \pm 1.4\%$. These values for P_c vs S_w have been complemented by more precise water-vapor physisorption measurements, presented below.

The SANS spectra of the wetted rock samples are depicted in Fig. 2, together with the SANS spectra of the

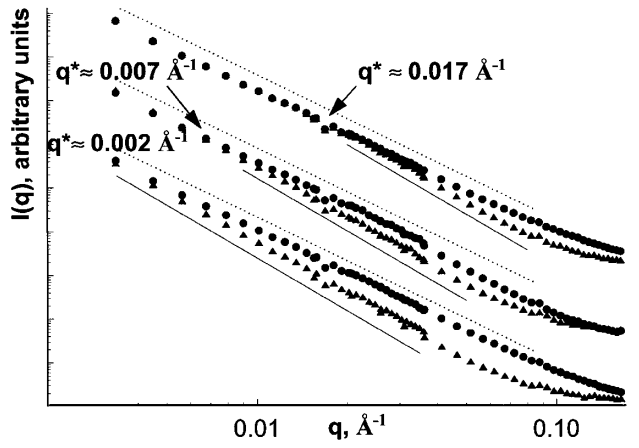

FIG. 2. SANS intensities of Vosges sandstones filled with a contrast-matched H_2O/D_2O fluid under a Kelvin capillary pressure (triangles), compared to the intensity of the dry medium (circles). From bottom to top, $P_c = 36$, 100, and 383 bars. Continuous lines have a slope of -4 (Porod) and dotted lines a slope of -3.32 ($D = 2.68$). The flattening at large q is due to the incoherent background, denoted B in Eq. (1).

corresponding dried samples. All wetted samples exhibited at large enough q a Porod scattering regime (q^{-4}) typical of flat (smooth) interfaces. This Porod regime crosses over at small q to the fractal scattering curve of the dried material. This crossover q^* is observed to move towards lower scattering vectors when the fluid content S_w increases, or, equivalently, when the capillary pressure in the medium decreases. For the sample containing the largest quantity of water (i.e., that obtained with a vapor of water saturated with K_2SO_4), the crossover lies outside the experimental window.

We find from these experiments that P_c/q^* is of the order of twice the surface tension of water ($\approx$73 dyn/cm), so that the Young-Laplace equation,

$$P_c = 2\gamma/R\,, \tag{4}$$

applies to our system, R being identified here to $1/q^*$. More precisely, $P_c/2q^*$ is equal to 72, 90, and 110 dyn/cm for $S_w \approx 14\%$, 12%, and 5%, respectively. This is evidence of a capillary wetting regime, with possibly increasing departure as S_w decreases. The wetting fluid occupies pores or surface concavities with radii of curvature smaller than $R \approx 1/q^*$, while all pores with radii $>R$ remain empty (except for some wetting films that make a negligible contribution to S_w). This threshold $R \approx 1/q^*$ increases with increasing fluid content in the porous medium. The pore space structure of the wetted porous medium has the same (fractal) distribution as the dried medium, but with a modified lower limit R (all pores with radii $<R$ being invisible in the scattering process). It is worth mentioning here the results of recent model calculations [11] for a fractal distribution of pores with a lower cutoff at some radius R: For small q ($>q^* \approx 1/R$), scattering is identical to that of the uncut distribution; while for large q ($>q^*$) scattering decreases similar to q^{-4}. In our experiments, the crossover scattering vector q^* between the fractal and Porod regimes can be identified with the curvature $1/R$ delineating large, empty asperities from small, filled asperities.

The wetting fluid distribution regime and the roughness (or fractal dimension) of the underlying porous medium are often inferred from measurements of capillary pressure or sorption isotherms. The existing models predict for these parameters very specific scaling dependences with the (low) porous medium filling S_w. In the capillary wetting regime, the capillary pressure behavior is deduced from Eq. (4) and from the relation between S_w and the characteristic length R, $S_w \approx R^{3-D}$ [6,12], leading to

$$P_c(S_w) \approx \frac{2\gamma}{R} \approx S_w^{-1/(3-D)}. \tag{5}$$

In the substrate-controlled wetting regime, capillary pressure obeys a different scaling behavior, even though there is a similar relation between fluid content and film thickness, $S_w \approx d^{3-D}$ [13]. In this regime, capillary pressure is dominated by the disjoining pressure of the film, i.e., if one assumes dominant van der Waals interactions

$$P_c(S_w) \approx -\frac{H}{d^3} \approx S_w^{-3/(3-D)}, \tag{6}$$

where $H > 0$ is the Hamaker constant of the wetting film. Theoretical expressions for the sorption isotherms in both regimes are obtained by replacing P_c in Eqs. (5) and (6) by the Kelvin pressure [Eq. (3)].

For the particular porous rock used for this study, previous measurements of the capillary pressure by mercury intrusion are consistent with a capillary wetting regime and a fractal dimension of the underlying rock $D \approx 2.7$; i.e., they verify Eq. (5) with $D \approx 2.7$ at low wetting phase (i.e., mercury vapor) content [14]. Sorption measurements usually display at low S_w a power-law behavior of the type described by Eqs. (5) and (6), with P_c the Kelvin pressure. However, the interpretation of such measurements is not straightforward, as the range of observed length scales [15] is often limited (usually not exceeding one decade), and as the fluid is often in an intermediate regime between capillary and substrate-controlled wetting [16]. In fact, crossover effects appear to be responsible for the observed lower fractal dimension D in sorption experiments [as inferred by Eq. (5)] as compared to D determined by small-angle scattering [17].

We have carried out water-vapor sorption measurements using the same porous media as those used for the small-angle scattering experiments. The whole adsorption and desorption cycles lasted more than two weeks, and the measurements were repeated twice. The results, depicted in Fig. 3 (where measured weights have been converted into S_w), exhibit a hysteresis between the adsorption and desorption cycles characteristic of capillary condensation. In addition, the behavior of both the adsorption and desorption branches at high relative pressure or coverage (P close to P_{sat}), plotted in the inset of Fig. 3, are consistent with an equation of the Frankel-Halsey-Hill–type, i.e.,

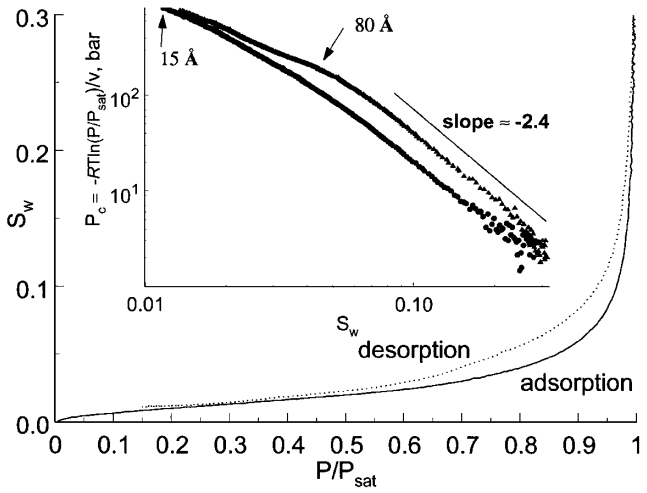

FIG. 3. Sorption data for water on the porous (crushed) sandstone. The inset is a representation to test Eqs. (5) and (6), with P_c given by Eq. (3).

$\log(P/P_{\rm sat}) = CS_w^{-p}$, with $p \approx 2.4$ and C being somewhat larger for desorption than for adsorption.

The use of Eq. (6) leads to an unphysical value for D ($D = 1.75 < 2$). The use of Eq. (5), on the other hand, leads to a fractal dimension $D \approx 2.58$, somewhat below the value determined from small-angle scattering data ($=2.68 \pm 0.03$). While this confirms that capillary wetting controls fluid distribution within the pore space, the underestimation of D, consistent with recent observations, shows the existence of crossover effects towards substrate-controlled wetting [17].

The length scales or distances [15] probed by these sorption experiments extend up to around 5000 Å ($P/P_{\rm sat} \approx 0.995$), which overlaps the domain investigated by SANS and SAXS. As is apparent in the inset of Fig. 3, the local slope p of the adsorption curve reaches the value 2.4 very progressively as $P/P_{\rm sat}$ increases, while there is a marked variation in the desorption curve for $S_w \approx 5\%$ (corresponding to relative pressures $P/P_{\rm sat} \approx 0.75$, or equivalent distances $\approx$80 Å), both curves merging for $S_w \approx 1\%$ ($P/P_{\rm sat} < 0.25$ and distances $R < 15$ Å, corresponding to the onset of capillary condensation). Departures from the capillary wetting behavior at low S_w are also apparent in the SANS results reported above, as well as in some other published desorption measurements in natural clay sandstones [18]. Such departures have been attributed to the dominance of films (substrate-controlled wetting); in this case, the dominant contribution to the film disjoining pressure cannot be van der Waals' $1/d^3$ term [cf. Eq. (6)], since one then would expect a steeper decay of P_c for $S_w < 5\%$ than for $S_w > 5\%$ (the opposite trend is observed experimentally) [12].

In conclusion, the contrast-matched SANS experiments presented in this Letter provide a direct visualization of wetting fluid distribution within a natural fractal porous medium. For this particular porous medium, both SANS and adsorption data indicate that capillary wetting is the dominant mechanism governing fluid (water) distribution, while some wetting film effects are present, especially for low fluid content (below around 5%). The wetting fluid has for effect to "defractalize" [7] the porous medium on the smaller length scales, in the sense that there is a new lower limit of the length scale of fractality, corresponding to the size of the largest filled pores. The fractal approach shows great promise in describing situations and quantities of engineering interest.

This work has been partially supported by a EC Joule Contract No. JOF3-CT97-0042. Laboratoire des Matériaux et Structures du Génie Civil is a Unité Mixte de Recherche LCPC-CNRS-ENPC.

*Corresponding author: daniel.broseta@ifp.fr

[1] A. P. Radlinski *et al.,* Phys. Rev. Lett. **82**, 3078 (1999).
[2] A. J. Katz and A. H. Thompson, Phys. Rev. Lett. **54**, 1325 (1985).
[3] P.-z. Wong, J. Howard, and J.-S. Lin, Phys. Rev. Lett. **57**, 637 (1986).
[4] H. D. Bale and P. W. Schmidt, Phys. Rev. Lett. **53**, 596 (1984); A. P. Radlinski and E. Z. Radlinska, in *Coalbed Methane: Scientific, Environmental and Economic Evaluation,* edited by M. Mastalerz, M. Glikson, and S. D. Golding (Kluwer, Dordrecht, 1999), pp. 329–365.
[5] P. Pfeifer and K.-Y. Liu, in *Equilibria and Dynamics of Gas Adsorption on Heterogeneous Solid Surfaces, Studies in Surface Science and Catalysis,* edited by W. Rudzinski, W. A. Steele, and G. Zgrablich (Elsevier, Amsterdam, 1997), Vol. 104, pp. 625–677.
[6] P. G. de Gennes, in *Physics of Disordered Materials,* edited by D. Adler, H. Fritsche, and S. R. Ovshinsky (Plenum, New York, 1985), pp. 227–241.
[7] E. Cheng, W. W. Cole, and P. Pfeifer, Phys. Rev. B **39**, 12 962 (1989).
[8] C. Durand, R. Szymanski, and J.-L. Renaud, Rev. I.F.P. **37**, 295 (1989).
[9] J. Teixeira, J. Appl. Cryst. **21**, 781 (1988).
[10] P.-z. Wong and A. J. Bray, Phys. Rev. Lett. **60**, 1344 (1988).
[11] A. P. Radlinski *et al.,* Org. Geochem. **31**, 1 (2000).
[12] H. T. Davis, Europhys. Lett. **8**, 629 (1989); H. T. Davis *et al.,* J. Phys. Condens. Matter **2**, SA457 (1990).
[13] P. Pfeifer *et al.,* Phys. Rev. Lett. **62**, 1997 (1989); E. Cheng, M. W. Cole, and A. Stella, Europhys. Lett. **8**, 537 (1989).
[14] F. Kalaydjian *et al.,* J. Pet. Sci. Eng. **17**, 275 (1997); J.-C. Moulu *et al.,* SPE Paper No. 38 891 (1997).
[15] The length scales or distances probed by a sorption experiment are given by Eqs. (3) and (4), i.e., $R = -2\gamma v/RT \log(P/P_{\rm sat})$.
[16] M. Kardar and J. O. Indekeu, Phys. Rev. Lett. **65**, 662 (1990); P. Pfeifer, M. W. Cole, and J. Krim, *ibid.* **65**, 663 (1990).
[17] J. Ma, H. Qi, and P.-z. Wong, Phys. Rev. E **59**, 2049 (1999); H. Qi, J. Ma, and P.-z. Wong, University of Massachusetts Report No. cond-mat/0010122.
[18] J. S. Ward and N. R. Morrow, Soc. Pet. Eng. Form. Eval. **2**, 345 (1987); J. C. Melrose, in *Characterization of Porous Solids,* edited by K. K. Unger *et al.* (Elsevier, Amsterdam, 1988).